



Biosynthesis of silver-based nanoparticles on polypropylene non-woven material for efficient antimicrobial activity

ANA G. KRKOBABIĆ¹, JOVANA D. STOJIČIĆ¹, MAJA M. RADETIĆ^{1*}
and DARKA D. MARKOVIĆ^{2**#}

¹University of Belgrade, Faculty of Technology and Metallurgy, Kardeljeva 4, 11120 Belgrade, Serbia and ²University of Belgrade, Innovation Centre of the Faculty of Technology and Metallurgy, Kardeljeva 4, 11120 Belgrade, Serbia

(Received 13 January, revised 23 February, accepted 9 April 2023)

Abstract: The outbreak of the COVID 19 pandemic confirmed the importance of personal protective equipment including the respiratory face masks as barriers to pathogens. Taking into account that face masks are mainly composed of polypropylene (PP) non-woven materials this study explores the possibility of *in situ* biosynthesis of silver-based nanoparticles as an antimicrobial agent on PP material. A pomegranate peel extract was used as a “green” agent for synthesis and stabilization of nanoparticles. Hydrophobicity of PP fibers was overcome by modification with corona discharge at atmospheric pressure. In order to improve the binding of silver ions, corona modified PP material was impregnated with biopolymer chitosan in the presence of crosslinker 1,2,3,4-butane-tetracarboxylic acid. SEM analysis revealed the presence of spherical Ag-based nanoparticles on the fiber surface with an average size of approximately 69 nm. The higher the concentration of the precursor salt, the higher the silver content after the reduction. Larger amounts of Ag-based nanoparticles provided stronger antimicrobial activity against bacteria *Escherichia coli* and *Staphylococcus aureus*, and yeast *Candida albicans*.

Keywords: pomegranate peel; chitosan; Ag nanoparticles; corona discharge.

INTRODUCTION

Until the outbreak of the COVID 19 pandemic, protective personal equipment including respiratory face masks has been mainly reserved for medical professionals but the years of living with SARS-CoV-2 virus stressed the importance of protective masks in everyday life.¹ Commonly used respiratory protective masks such as N95 and KN95 are composed of multiple layers of polypropylene (PP) non-woven material. In general, PP non-woven materials are widely used in

* Corresponding author. E-mail: darka@tmf.bg.ac.rs

Serbian Chemical Society member.

<https://doi.org/10.2298/JSC230113020K>

medical textiles as a part of personal protective equipment like facemasks, disposable surgical gowns, drapes, shoe covers, head covers, etc.² Keeping in mind that PP fibers do not provide any antimicrobial activity, protective masks can only act as a physical barrier to pathogens transmission but they are not able to inactivate pathogens.¹ Furthermore, the probability of pathogen penetration through the mask increases with wearing time.^{1,3} To overcome the possible contamination of users, frequent change of mask is recommended, but this is not economically and environmentally acceptable. Moreover, properties of PP fibers and fabrication method of face masks do not allow the efficient sterilization for re-use by standard methods in disinfect solutions.^{1,3,4} These shortcomings of personal protective equipment are particularly common in hospital environment where transmission of pathogens from patients to personnel and *vice versa* induces additional spreading of hospital infections.⁵

A variety of antimicrobial agents have been tested for possible application to PP non-woven materials.^{6–12} Extraordinary antimicrobial activity against *E. coli*, *S. aureus* and *C. albicans* is obtained by impregnation of PP non-woven material with thymol using supercritical CO₂.⁶ During the pandemic of fly influence A H1N1, Borkov *et al.* discovered that respiratory protective face masks impregnated with copper oxide showed influenza biocidal properties without change of physical barrier properties.⁷ Excellent antimicrobial activity is also obtained by *in situ* synthesis of copper oxide nanoparticles on PP non-woven material using ascorbic acid as a reducing agent.⁸ Coating of protective mask with a thin layer of copper film results in the reduction of virus SARS-CoV-2 by more than 75 %.⁹ Kumar *et al.* reported that face masks coated with copper nanoparticles could provide significant protection from SARS-CoV-2 transmission.¹⁰ Promising method for imparting biocide activity to N95 facemasks proposes simultaneous polymerization and grafting of C12-quaternized benzophenone using a UV irradiation.¹ Nanostructured silver films successively deposited on the surface of PP non-wovens by magnetron sputter coating provides satisfactory antibacterial activity.¹¹ Good antimicrobial activity is also achieved by *in situ* synthesis of silver nanoparticles on PP material with glucose as a reducing agent.¹²

Modification of PP non-woven material is a big challenge for scientists because of chemical inertness and hydrophobicity of PP fibers. To overcome this problem, many authors proposed the deposition of active agents like copper oxide or silver onto PP surface using magnetron sputter coating systems.^{9,11} Kumar and co-workers designed special microfluidic 3D spray device for depositing the nanocomposite layer onto a non-woven mask.¹⁰ The deposition of quaternary ammonium salts by dissolving them in acetone and then exposing to 254 nm UV light to initiate benzophenone cross-linking is also proposed.¹ The activation of PP surface by corona discharge at atmospheric pressure before further processing is another efficient approach.⁸ Namely, plasma oxidation

results in introduction of polar groups on the fiber surface improving the hydrophilicity and reactivity, and facilitating the further coating with biopolymer alginate and copper oxide nanoparticles.⁸

In the current study, corona discharge is applied for the activation of PP non-woven material prior to coating with biopolymer chitosan in the presence of crosslinker 1,2,3,4-butanetetracarboxylic acid. Chitosan, which is non-toxic, biocompatible, biodegradable, was selected due to its affinity to heavy metal ions, and thus to Ag-ions.¹³ To keep in line with environmental friendless and follow the trends in the synthesis of metal-based nanoparticles (NPs), a waste pomegranate peel (*Punica granatum*) was used as a green agent for the synthesis of Ag-based NPs. Pomegranate peel is rich in various polyphenolic compounds, which act as stabilizing agent. The influence of the concentration of silver nitrate as a precursor salt on antimicrobial activity of textile nanocomposite against Gram-negative bacteria *E. coli*, Gram-positive bacteria *S. aureus* and yeast *C. albicans* was explored. To the best of our knowledge there are no literatures data dealing with biosynthesis of Ag-based NPs using pomegranate peels extract onto PP nonwoven material modified with cross-linked chitosan.

EXPERIMENTAL

Modification of PP non-woven material

PP non-woven material cleaned with ethanol (Zorka Pharma) was treated with corona discharge at atmospheric pressure using a commercial device Vetaphone CP-Lab MK II. The sample was placed on the electrode roll covered with silicon coating, rotating at the minimum speed of 4 m/min. The power was set to 700 W, the number of passages was 30 and the distance between the electrodes was 2.2 mm. This sample is denoted CPP.

CPP fabric was further treated with biopolymer chitosan (CH, ChitoClear®, source: *Pandalous borealis*, Primex, deacetylation degree of 90 % and viscosity of 847 mPa·s,) with or without 1,2,3,4-butanetetracarboxylic acid (BTCA, Acros Organics). A CH solution was prepared by dissolving 1.00 g of CH in 100 mL of 1 vol. % acetic acid (Zorka Pharma), which was stirred at room temperature for 24 h. In order to eliminate the gas bubbles formed during the agitation, the solution was left to settle for 30 min.

CPP sample of 0.50 g was immersed in 75 mL of freshly prepared CH solution and left for 1 h at the room temperature. After padding (1 kg cm⁻³), the sample was dried at 80 °C for 8 min, rinsed with distilled water and left to dry at room temperature. This sample is denoted CPP_CH.

The coating in the presence of BTCA was performed using the following procedure: 2 % of BTCA and 1.2 % of sodium hypophosphite (SHP, Acros Organics) as a catalyst were added to 75 mL of prepared CH solution. After being immersed in 75 mL of freshly prepared solution for 1 h, the sample was padded, dried at 80 °C for 5 min and cured at 120 °C for 3 min. Dry sample was then rinsed with distilled water and left to dry at room temperature. This sample is denoted CPP_CHB.

CPP sample (0.50 g) was also treated with 75 mL of 2 % BTCA solution in the presence of 1.2 % of SHP. This sample is denoted CPP_B.

Extraction of reducing agent and in situ biosynthesis of Ag-based NPs

Pomegranate peel was collected and further grinded in the Institute for Medical Plant Research “Dr Josif Pančić” (Serbia). 5 % water extract was prepared at 80 °C within 1 h. Extract was subsequently filtered and used for the synthesis of Ag nanoparticles.

CPP_B, CPP_CH and CPP_CHB (0.50 g) were immersed in 30 mL of 10 and 20 mM solution of AgNO₃ for 2 h and then rinsed with distilled water. The synthesis of Ag-based NPs was conducted in 30 mL of pomegranate peel extract at 60 °C for 1 h. The samples were thoroughly rinsed with distilled water and dried at room temperature. The samples obtained from 10 mM AgNO₃ solution are denoted CPP_B_Ag10, CPP_CH_Ag10 and CPP_CHB_Ag10. In the same manner the samples synthesized from 20 mM AgNO₃ solution are denoted CPP_B_Ag20, CPP_CH_Ag20 and CPP_CHB_Ag20. CPP_CHB sample treated only with pomegranate peel extract is denoted CPP_CHB_P. The whole procedure is illustrated in Fig. 1.

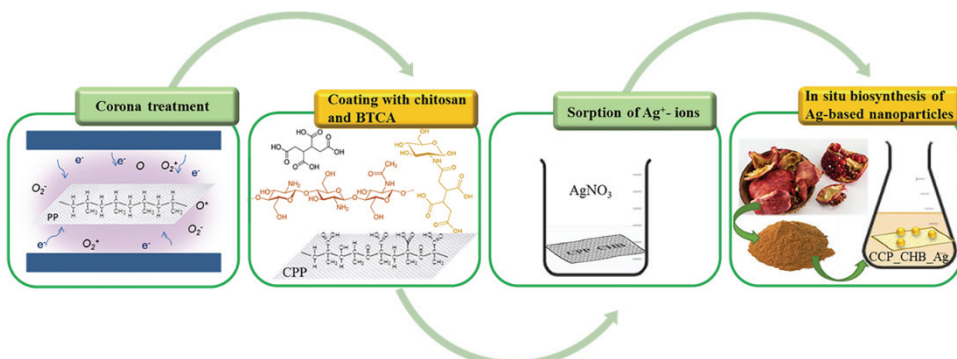


Fig. 1. Schematic illustration of proposed procedure.

Characterization of synthesized materials

The morphology of the samples along with the qualitative analysis of chemical composition and distribution of silver over the surface was investigated by field emission scanning electron microscopy equipped with an energy dispersive X-ray spectrometer (FESEM-EDS, FEI SCIOS 2 Dual Beam). The samples were recorded under high vacuum with an acceleration voltage of 7 keV, while the EDS mapping acquisition time was 30 min. The size and size distribution of NPs were analyzed using the open-access imaging software tool ImageJ.

The Ag⁺ uptake on CPP_CHB_Ag10 and CPP_CHB_Ag20 from AgNO₃ solution was calculated on the basis of the concentration of residual Ag⁺ in the solution which was measured using a Spectra AA 55 B (Varian) atomic absorption spectrometer (AAS). The Ag⁺ uptake (*q*) was calculated as:

$$q = \frac{V(C_{Ag_0} - C_{Ag})}{m} \quad (1)$$

where *C_{Ag}0* is the initial concentration of Ag⁺ in the solution (mol L⁻¹), *C_{Ag}* is the concentration of Ag⁺ in the solution after 2 h long adsorption (mol L⁻¹), *V* is the volume of the AgNO₃ solution (L) and *m* is the weight of the fabric (g).

AAS was also applied for measuring the total Ag content in the materials after reduction. The samples were solved in 1:1 HNO₃ solution. The experiments were done in triplicate.

Color coordinates (CIE L^* , a^* , b^*) of the fabrics were determined by spectrophotometer (Datacolor SF300, USA) under illuminant D65 using the 10° standard observer. On the basis of measured CIE color coordinates, the color difference (ΔE^*) between the fabrics before and after the synthesis of Ag NPs was determined as:

$$\Delta E^* = \sqrt{(\Delta a^*)^2 + (\Delta b^*)^2 + (\Delta L^*)^2} \quad (2)$$

where: ΔL^* – the lightness difference; Δa^* – red/green difference; Δb^* – yellow/blue difference.

Fourier transform infrared (FTIR) spectra of control and synthesized samples were recorded in the ATR mode using a Nicolet iS5 FTIR spectrometer (Thermo Scientific) at 2 cm⁻¹ resolution, in the wavenumber range 500–4000 cm⁻¹.

The wettability of the samples was studied using a thin-layer wicking test of wettability (TLW) which was carried out in the horizontal direction according to Chibowski and Gonzales-Caballero.¹⁴ The samples were cut into strips (1 cm×10 cm) and dried for 30 min at 100 °C. Each dry sample was inserted between two glass plates with a ruler and carefully put into touch with deionized water in a Petri dish. Starting from the moment when the water began to penetrate into the fabric sample, the time at which the water penetrated a certain distance in the fabric was measured. For each fabric sample, at least 10 measurements were made, and the average value was presented as a result.

The antimicrobial activity of PP samples modified with Ag-based nanoparticles was tested against Gram-negative bacteria *E. coli* ATCC 25922, Gram-positive bacteria *S. aureus* ATCC 25923 and fungi *C. albicans* ATCC 24433, using a standard test method for determination of the antimicrobial activity of immobilized antimicrobial agents under dynamic contact conditions ASTM E 2149-01 (2001). Microorganisms were cultivated in 3 mL of tryptone soy broth (supplemented with 0.6 % of yeast extracts) at 37 °C in thermostat for 18 h (late exponential stage of growth). 50 mL of sterile physiological saline solution was subsequently inoculated with 0.5 mL of microbial inoculum. One gram of each sample, control and impregnated with particles, was sterilized in autoclave (30 min) and placed into a flask (with sterile physiological saline solution and inoculum) that was shaken at 37 °C for 2 h. 1 mL aliquots from the flask were taken for viable cell determination and put (1 mL) in a Petri dish on the tryptone soy agar (with 0.6 % yeast extracts). The Petri dishes were incubated at 37 °C for 24 h. After 24 h of incubation at 37 °C, zero-time (inoculum) and two-hour counts of viable microorganisms were made. The percentage of microbial reduction (R , %) was calculated in accordance with the following equation:

$$R = 100 \frac{C_0 - C}{C_0} \quad (3)$$

where C_0 (CFU – colony forming units) is the number of microorganism colonies on the control fabric and C (CFU) is the number of microorganism colonies on the fabric impregnated with Ag particles. Number of microorganism's colonies was expressed as colony forming units in 0.1 mL aliquots. The experiments were done in triplicate.

In an attempt to evaluate the leaching of Ag⁺ from the samples, impregnated fabrics were dipped into physiological saline solution (9 g L⁻¹ NaCl) and left to rest at temperature of 37 °C for 1, 3, 6 and 24 h. The concentration of released Ag⁺ was measured after 1, 3, 6 and 24 h by AAS. The experiments were done in triplicate.

RESULTS AND DISCUSSION

Taking into account that corona treatment leads to activation of PP fibers surface, *i.e.*, creation of polar groups in the polymer chain, the first step in the current study was to examine if newly formed polar groups only altered the fiber surface hydrophilicity or they could be potential sites for binding of Ag^+ . The preliminary results confirmed that corona activation of PP non-woven material brought about significantly improved hydrophilicity. Biosynthesis of Ag-based NPs is commonly followed by color change (yellow shades) of textile substrates. The lack of color change of CPP samples after the synthesis of Ag-based NPs pointed out that the synthesis of NPs did not occur. In other words, corona activation did not provide adequate active groups for binding of Ag^+ . The next step was to select an environmentally benign agent that can provide desirable active groups for the sorption of Ag^+ . The ability of biopolymer chitosan to form the complexes with heavy metal ions was utilized for modification of CPP non-woven material. Amino groups of chitosan enhanced the binding of Ag^+ and consequently the substrates changed the color to yellow shades after the NPs synthesis step with bio-extract. A distinct color unevenness of obtained sample indicated insufficiently efficient coating of CPP sample with chitosan. In order to improve the coating of CPP samples, chitosan was eventually applied in the presence of BTCA as a crosslinking agent. Fig. 2a shows that such modification produces uniform color of the samples suggesting that BTCA enhances the binding of chitosan to fibers. Fig. 2a also illustrates three successive synthesis steps through the color change. Namely, after the adsorption of Ag^+ , as expected, the samples retained white. After the synthesis step in the presence of pomegranate peel extract, the color was changed to ocher and finally, after drying the samples, became brownish. Evident color changes confirm the formation of Ag-based NPs.^{15–17}

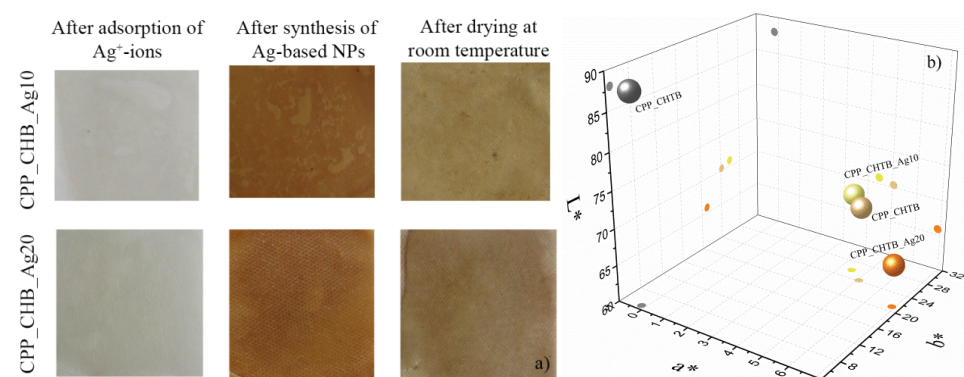


Fig. 2. Color change of the samples during the synthesis of nanoparticles: a) photographs of the samples after each step of *in situ* biosynthesis and b) CIE L^* , a^* , b^* coordinates.

The results of objective quantification of color change are presented in Fig. 2b and Table I. Compared to control sample, the samples impregnated with Ag⁺-based NPs are significantly darker. This is particularly pronounced in the sample where 20 mM AgNO₃ solution was applied. A large color difference ($\Delta E^* = 7.46$) between CPP_SHB_Ag10 and CPP_CHB_Ag20 indicates that the concentration of precursor salt strongly affects the amount of synthesized Ag-based NPs and consequently, the color of the samples. Evident color changes are in line with AAS analysis (Table II), which shows that higher concentration of AgNO₃ solution causes larger Ag⁺ uptake and higher total content of silver in the samples. The difference between the values of initial uptake and the total content of silver (Table II) is suggested to be due to the reduction processes ran at higher temperature. Such trend is already described in literature.¹⁷

TABLE I. CIE L^* , a^* , b^* differences between the samples

Control	Sample	ΔE^*	ΔL^*	Δa^*	Δb^*	Descriptions
CPP	CPP_CHB_P	26.6	-17.6	5.23	19.26	Darker, less green, yellow
	CPP_CHB_Ag10	27.4	-17.0	4.63	30.0	Darker, less green, yellow
	CPP_CHB_Ag20	28.3	-22.1	7.01	16.1	Darker, less green, yellow
CPP_CHB_Ag10	CPP_CHB_Ag20	7.46	-5.09	2.45	-4.87	Darker redder less yellow

TABLE II. Ag⁺ uptake and total content of silver in the samples

Sample	Ag ⁺ uptake, $\mu\text{mol g}^{-1}$	Total content of silver after reduction, $\mu\text{mol g}^{-1}$
CPP_CHB_Ag10	10.44±0.84	4.10±0.10
CPP_CHB_Ag20	35.24±0.13	7.69±0.13

Chemical changes induced by corona and chitosan treatment are evaluated by FTIR spectroscopy. FTIR spectra of PP, CPP and CPP_CHB samples are shown in Fig. 3. The spectrum of PP non-woven fabric reveals all characteristic bands for PP: CH₃ and CH₂ asymmetric and symmetric stretching vibrations (2950–2830 cm^{-1}), CH₃ asymmetric deformation vibrations or CH₂ scissor vibrations and CH₃ symmetric deformation vibrations (1457–1356 cm^{-1}) and vibrations associated with C–C bonding (1200–800 cm^{-1}).^{18,19} Corona treatment results in creation of two new bands at 1720 and 1636 cm^{-1} . The absorption band at 1720 cm^{-1} is ascribed to carbonyl groups in aldehydes and ketones, respectively. The band at 1636 cm^{-1} is likely due to COO[−] asymmetric stretching vibrations.^{18,19} Coating with chitosan led to decrease in intensity of the band at 1720 cm^{-1} along with significant decrease in the intensity of band at 1636 cm^{-1} . Additionally, a new band at 1555 cm^{-1} attributed to vibration in secondary amide appeared.^{20,21} The appearance of this band implies that amide groups are formed between the amino groups of chitosan and carboxyl group of BTCA. A broad

band between 3225-3350 cm⁻¹, that is pronounced in CPP_CHB spectra, is ascribed to asymmetric stretching vibrations of –NH₂ or –OH groups.²¹

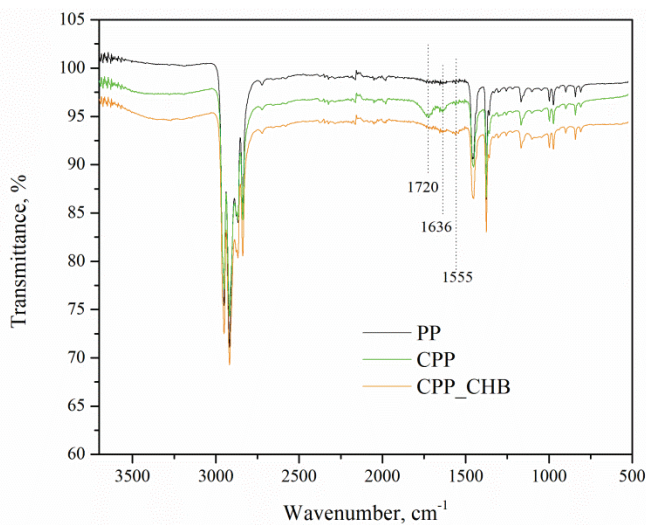


Fig. 3. FTIR spectra of the samples after modification with corona and chitosan.

In addition to chemical changes, corona treatment causes morphological changes on the PP fibers surface. FESEM micrograph shows that corona discharge creates the holes (Fig. 4b) on the flat surface of PP fibers (Fig. 4a). This is in line with our previous observation.⁸ Fig. 4c reveals that spherical Ag-based NPs with an average size of 69±17 nm are synthetized on the surface of CPP_CHB_Ag20 sample pointing out that waste pomegranate peels could be successfully exploited for the synthesis of NPs. It is reported that pomegranate peel extract consists on punicalagin and punicalin components, that belong to the group of ellagatannins containing 16 and 10 phenolic hydroxyls per molecule, respectively.¹⁶ Polyphenols can act as reducing and stabilizing agents to some metal ions.²² XPS analysis revealed that use of pomegranate peels for *in situ* biosynthesis of Ag-based NPs results in the formation of AgCl NPs.¹⁶ Other researchers also suggested that that AgCl is the most typical compound found in final product of plant-mediated synthesis of Ag NPs.^{23,24} Fig. 4c shows EDX element distribution mapping of CPP_CHB_Ag20 surface. Different colors were used to visually distinguish the presence of carbon (red), nitrogen (green), oxygen (cyan), chlorine (violet) and silver (yellow). Besides carbon and oxygen, the obtained maps indicate that nitrogen along with chlorine and silver uniformly covered the fiber surface. The regions with a larger silver content were found to approximately coincide with those covered with chlorine indicating that NPs might be synthesized in the form of AgCl, which is in line with literature.^{15,16,23,24} Namely,

AgCl is the most typical compound detected in the final product of plant-mediated synthesis of Ag NPs.^{23,24} A size distribution of NPs (Fig. 4d) demonstrates that significant number of particles, synthetized on the CPP_CHB_Ag20 surface, are in the range between 30 and 90 nm.

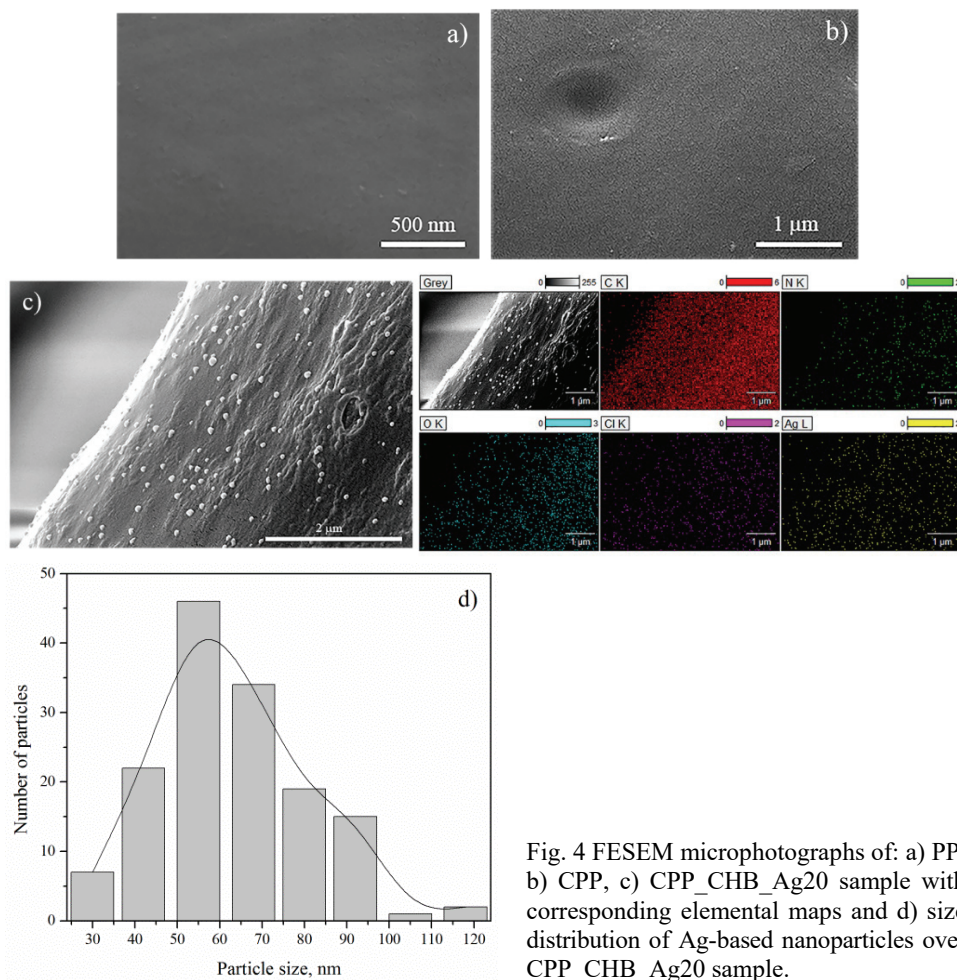


Fig. 4 FESEM microphotographs of: a) PP, b) CPP, c) CPP_CHB_Ag20 sample with corresponding elemental maps and d) size distribution of Ag-based nanoparticles over CPP_CHB_Ag20 sample.

As already mentioned, corona treatment was performed to improve the hydrophilicity of PP fibers. Thin-layer wicking test cannot be applied for evaluation of the control PP material as it is highly hydrophobic. Simple drop test showed that PP non-woven fabric became immediately wet after corona treatment. Coating with biopolymer chitosan diminished the effect obtained with corona (Fig. 5), but the material can be still considered as hydrophilic because the wetting time measured by drop test was less than 2 min. It is interesting to note that the coat-

ing of CPP fibers with biopolymer alginate also has a negative influence on the fiber surface hydrophilicity.⁸ Synthesis of Ag-based NPs positively affected the material hydrophilicity compared to CPP_CHB sample. The difference between CPP_CHB_Ag10 and CPP_CHB_Ag20 samples as a consequence of the total content of Ag was observed once again. CPP_CHB_Ag10 sample demonstrated better hydrophilicity than CPP_CHB_Ag20 sample.

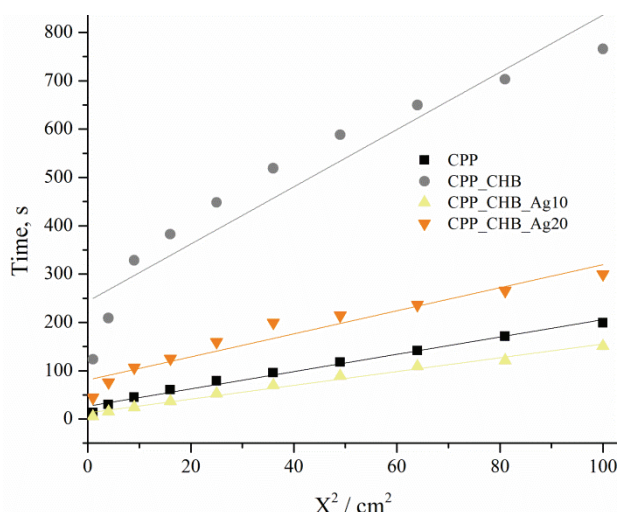


Fig. 5. Rate (X^2/time) of thin-layer wicking of water into investigated samples.

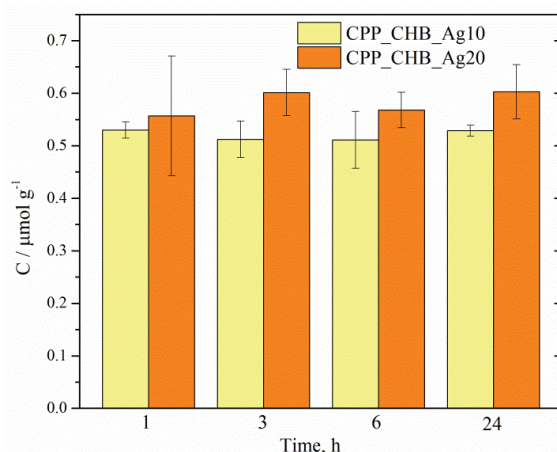
Finally, the main reason for the synthesis of Ag-based NPs was to impart antimicrobial activity to PP non-woven material. The three most frequently tested pathogens were selected for investigation of antimicrobial activity of synthesized samples. The results, summarized in Table III, reveal that both samples provided excellent antimicrobial activity against Gram-positive bacteria *S. aureus* and yeast *C. albicans*. In the case of Gram-negative bacteria *E. coli* moderate antibacterial activity was obtained. The larger the amount of silver in the samples, the better the antimicrobial activity. It should be emphasized that CPP, CPP_CHB and CPP_CHB_P samples did not provide any antimicrobial activity against tested strains. Although the antimicrobial action of Ag NPs has been widely investigated for a long-time, the exact mechanism of their antimicrobial action has not been completely resolved yet. It is supposed that the combination of various processes such as attack of cell membrane by Ag^+ released from Ag NPs, metal–microorganism contact, generation of ROS, *etc.*, leads to cells death.^{24,25}

The possible release of silver was assessed in the physiological saline solution. Physiological saline solution was selected to simulate the body fluids. Fig. 6 presents the dependence of released amount of Ag^+ on time. A similar amounts of Ag^+ were released from the sample independently of time. Again, the higher

the total silver content, the larger the amount of released Ag^+ . Taking into account the results from Table II, it is clear that after the release study approximately 87 and 92 % of silver retained in the CPP_CHB_Ag10 and CPP_CHB_Ag20 samples, respectively. Since the released amount of Ag^+ did not change significantly over time, it could be assumed that stable nanocomposite was obtained.

TABLE III. Antimicrobial activity of samples with Ag-based NPs

Sample	Microorganism					
	<i>E. coli</i>		<i>S. aureus</i>		<i>C. albicans</i>	
	CFU	R / %	CFU	R / %	CFU	R / %
Inoculum	8.5×10^5	—	9.2×10^4	—	1.3×10^5	—
PP	6.6×10^5	—	4.0×10^4	—	8×10^4	—
CPP_CHB_Ag10	7.0×10^4	89.3	185	99.5	1.2×10^3	98.5
CPP_CHB_Ag20	2.8×10^4	95.8	20	99.9	800	99.0

Fig. 6. Release study of Ag^+ from sample in physiological saline solution.

Moreover, the amount of released Ag^+ is very important from the cytotoxicity point of view since cytotoxicity of metal-based NPs have been thoroughly investigated over the last decade. Results from Fig. 6 implied that maximum amount of released Ag^+ was about $0.7 \mu\text{mol g}^{-1}$ within 24 h. According to our previous studies and literature data, detected amount of released Ag^+ could be considered as safe for human skin cells.^{15,26,27}

CONCLUSION

Antimicrobial PP non-woven materials can be efficiently produced by proposed green synthesis procedure, which includes: *i*) activation of PP fibers by corona discharge at atmospheric pressure, *ii*) coating with biopolymer chitosan in the presence of BTCA and *iii*) *in situ* biosynthesis of Ag-based nanoparticles

using pomegranate peel extract as stabilizing agent. Each synthesis step induces change in color, hydrophilicity and surface chemistry of fibers. FESEM micrograph revealed that surface of PP fibers was covered with spherical nanoparticles implying that applied extract can be successfully used as a green agent for synthesis of Ag-based nanoparticles. Larger amounts of silver were synthesized with higher concentrations of precursor salt. Developed nanocomposite material provides a good antimicrobial protection against *S. aureus* and *C. albicans* with small quantity of released ions into physiological saline solution.

Acknowledgement. This work was financially supported by the Ministry of Science and Technological Development and Innovation of the Republic of Serbia (Contracts No. 451-03-47/2023-01/200135 and 451-03-47/2023-01/200287).

ИЗВОД

БИОСИНТЕЗА НАНОЧЕСТИЦА НА БАЗИ СРЕБРА НА НЕТКАНОМ ПОЛИПРОПИЛЕНСКОМ МАТЕРИЈАЛУ ЗА ЕФИКАСНУ АНТИМИКРОБНУ АКТИВНОСТ

АНА Г. КРКОБАБИЋ¹, ЈОВАНА Д. СТОИЧИЋ¹, МАЈА М. РАДЕТИЋ¹ и ДАРКА Д. МАРКОВИЋ²

¹Универзитет у Београду, Технолошко-мешалурски факултет, Карнејијева 4, 11120 Београд и

²Универзитет у Београду, Иновациони центар Технолошко-мешалуршког факултета,
Карнејијева 4, 11120 Београд

Појавом COVID 19 пандемије је потврђена важност употребе личне заштитне опреме као што су респираторне маске које пружају физичку заштиту од патогених сојева микроорганизама. Имајући у виду да се заштитне маске углавном производе од нетканог материјала од полипропиленских влакана, у овом раду је испитана могућност *in situ* биосинтезе наночестица на бази сребра као антимикробног средства на полипропиленском материјалу. Екстракт од коре нара је употребљен као „зелено“ средство за синтезу наночестица. Хидрофобност полипропиленских влакана је превазиђена њиховом модификацијом корона пражњењем на атмосферском притиску. У циљу побољшања везивања јона сребра, полипропиленски материјал модификован короном је импрегниран биополимером хитозаном у присуству умреживача 1,2,3,4-бутантетракарбоксилне киселине. ФЕСЕМ анализом је потврђено присуство сферних наночестица на површини влакана, просечних димензија око 69 nm. Већа концентрација раствора соли прекурсора доприноси већем садржају сребра након редукције. Веће количине честица на бази сребра обезбедиле су снажнију антимикробну активност према бактеријама *Escherichia coli* и *Staphylococcus aureus* и квасцу *Candida albicans*.

(Примљено 12. јануара, ревидирано 23. фебруара, прихваћено 9. априла 2023)

REFERENCES

1. M. Sorci, T. D. Fink, V. Sharma, S. Singh, R. Chen, B. L. Arduini, K. Dovidenko, C. L. Heldt, E. F. Palermo, R. H. Zha, *ACS Appl. Mater. Interfaces* **14** (2022) 25135 (<https://doi.org/10.1021/acsami.2c04165>)
2. D. Markovic, S. Milovanovic, M. Radetic, B. Jokic, I. Zizovic, *J. Supercrit. Fluids* **101** (2015) 215 (<https://doi.org/10.1016/j.supflu.2015.03.022>)
3. L. Liao, W. Xiao, M. Zhao, X. Yu, H. Wang, Q. Wang, S. Chu, Yi Cui, *ACS Nano* **14** (2020) 6348 (<https://dx.doi.org/10.1021/acsnano.0c03597>)

4. J. S. Smith, H. Hanseler, J. Welle, R. Rattray, M. Campbell, T. Brotherton, T. Moudgil, T. F. Pack, K. Wegmann, S. Jensen, J. Jin, C. B. Bifulco, S. A. Prahl, B. A. Fox, N. L. Stucky, *J. Clin. Translat. Sci.* **5** (2020) 1 (<https://dx.doi.org/10.1017/cts.2020.494>)
5. A. Kramer, I. Schwebke, G. Kampf, *BMC Infectious Diseases* **6** (2006) 130
6. Y. Gao, R. Cranston, *Text. Res. J.* **78** (2008) 60
7. G. Borkow, S. Zhou, T. Page, J. Gabbay, *PLoS One* **5** (2010) e11295 (<https://doi.org/10.1371/journal.pone.0011295>)
8. D. Marković, H. H. Tseng, T. Nunney, M. Radoičić, T. I. Tomic, M. Radetić, *Appl. Surf. Sci.* **527** (2020) 146829 (<https://doi.org/10.1016/j.apsusc.2020.146829>)
9. S. Jung, J. Y. Yang, E. Y. Byeon, D. G. Kim, D. G. Lee, S. Ryoo, S. Lee, C. W. Shin, H. W. Jang, H. J. Kim, S. Lee, *Polymer* **13** (2021) 1367 (<https://doi.org/10.3390/polym13091367>)
10. S. Kumar, M. Karmacharya, S. R. Joshi, O. Gulenko, J. Park, G. H. Kim, Y. K. Cho, *Nano Lett.* **21** (2021) 337 (<https://doi.org/10.1021/acs.nanolett.0c03725>)
11. H. Wang, J. Wang, J. Hong, Q. Wei, W. Gao, Z. Zhu, *J. Coat. Technol. Res.* **4** (2007) 101 (<https://doi.org/10.1007/s11998-007-9001-8>)
12. S. M. Gawish, S. Mosleh, *Fiber. Polym.* **21** (2020) 19 (<https://dx.doi.org/10.1007/s12221-020-9519-2>)
13. P. Wei, H. Lou, X. Xu, W. Xu, H. Yang, W. Zhang, Y. Zhang, *Appl. Surf. Sci.* **539** (2021) 148195 (<https://doi.org/10.1016/j.apsusc.2020.148195>)
14. E. Chibowski, F. Gonzales-Caballero, *Langmuir* **9** (1993) 330 (<https://doi.org/10.1021/la00025a062>)
15. N. Shreyash, S. Bajpai, M. A. Khan, Y. Vijay, S. K. Tiwary, M. Sonker, *ACS Appl. Nano Mater.* **4** (2021) 11428 (<https://doi.org/10.1021/acsanm.1c02946>)
16. A. Krkobabić, M. Radetić, H.H. Tseng, T. S. Nunney, V. Tadić, T. Ilic-Tomic, D. Marković, *Appl. Surf. Sci.* **611** (2023) 155612 (<https://doi.org/10.1016/j.apsusc.2022.155612>)
17. A. Krkobabić, D. Marković, A. Kovačević, V. Tadić, M. Radoičić, T. Barudžija, T. Ilic-Tomic, M. Radetić, *Fiber. Polym.* **22** (2022) 954 (<https://doi.org/10.1007/s12221-022-4639-5>)
18. R. Morent, N. de Geyter, C. Leys, L. Gengembre, E. Payen, *Text. Res. J.* **77** (2007) 471 (<https://doi.org/10.1177/0040517507080616>)
19. K.G. Kostov, T.M.C. Nishime, L.R.O. Hein, A. Toth, *Surf. Coat. Technol.* **234** (2013) 60 (<https://doi.org/10.1016/j.surfcoat.2012.09.041>)
20. R. Molina, P. Jovancic, S. Vilchez, T. Tzanov, C. Solans, *Carbohydr. Polym.* **103** (2014) 472 (<https://doi.org/10.1016/j.carbpol.2013.12.084>)
21. S. Rashid, C. Shen, X. Chen, S. Li, Y. Chen, Y. Wen, J. Liu, *RSC Adv.* **5** (2015) 90731 (<https://doi.org/10.1039/c5ra14711e>)
22. S. Eslami, M. A. Ebrahimzadeh, P. Biparva, *RSC Adv.* **8** (2018) 26144 (<https://doi.org/10.1039/c8ra04451a>)
23. N. Durán, G. Nakazato, A.B. Seabra, *Appl. Microbiol. Biotechnol.* **100** (2016) 6555 (<https://doi.org/10.1007/s00253-016-7657-7>)
24. V. Ravichandran, S. Vasanthi, S. Shalini, S.A.A. Shah, M. Tripathy, N. Paliwal, *Results Phys.* **15** (2019) 102565 (<https://doi.org/10.1016/j.rinp.2019.102565>)
25. J.P. Ruparelia, A.K. Chatterjee, S.P. Duttagupta, S. Mukherji, *Acta Biomater.* **4** (2008) 707 (<https://doi.org/10.1016/j.actbio.2007.11.006>)

26. Q. Xu, R. Li, L. Shen, W. Xu, J. Wang, Q. Jiang, L. Zhang, F. Fu, Y. Fu, X. Liu, *App. Surf. Sci.* **497** (2019) 143673 (<https://doi.org/10.1016/j.apsusc.2019.143673>)
27. A. I. Ribeiro, V. Shvalya, U. Cvelbar, R. Silva, R. M. Oliveira, F. Remião, H.P. Felgueiras, J. Padrão, A. Zille, *Polymers* **14** (2022) 1138 (<https://doi.org/10.3390/polym14061138>).